# Radiation in the Near Zone of a Short Center-Fed Biconical Antenna

Kirk T. McDonald
*Joseph Henry Laboratories, Princeton University, Princeton, NJ 08544*
(June 14, 2004)

# 1 Problem

The electromagnetic fields far from any antenna can be conveniently described as the sum of the radiation fields of a series of oscillating point multipoles, of which the leading term is a dipole in many cases of practical interest. The form of the fields associated with the $n$th multipole is independent of the details of the physical layout of the antenna (other than that the layout determines the magnitudes of the multipole moments). However, close to the antenna the electromagnetic fields include quasistatic components as well as radiation terms. A well-known argument due to Hertz [1, 2] gives the fields in the near and far zone of an ideal point dipole. In this and companion notes [3, 4] we explore examples in which analytic expressions can be given for the near and far zone fields of antennas of finite dimensions.

Here, the task is to describe the electromagnetic fields, and the Poynting vector [5], produced by oscillating currents of angular frequency $\omega$ that flow along the generators of a pair of opposing, perfectly conducting cones of half angle $\theta_0$ and length $a$. For a short antenna, $ka = k\omega/c \ll 1$. The cones have a common axis and meet at their vertices, as shown in the figure below (from [6]). The cones are excited by a voltage $V = V_0 e^{-i\omega t}$ applied across the gap between the two vertices. The resulting current along the surface of the cone is assumed to be independent of the azimuth around the cones. The currents are fed from the center of the antenna (tips of the cones) by, say, a coaxial feed line.

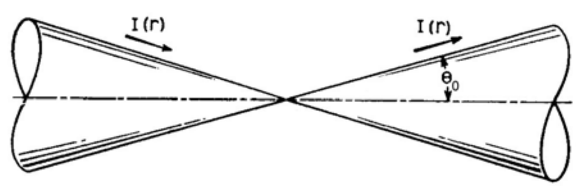


# 2 Solution

This problem is based on the work of Schelkunoff [6, 7] who noted that a difficulty in analytic modeling of linear antennas with finite-diameter wires is the resulting large capacitance between the pair of wires where they attach to the feed lines. The approximation of conical rather than cylindrical wires permits analytic calculations to proceed at only a modest loss of realism.[1]

We note immediately that a perfect conductor can only support an electric field perpendicular to its surface. Hence, the Poynting vector cannot be perpendicular to the surface of

[1] A brief discussion of biconical antennas is given in sec. 12.07 of [8].

a perfect conductor. Net electromagnetic energy can flow past the surface of perfect conductor, parallel to that surface, but net energy cannot be emitted or absorbed by such a surface. Of course, a perfect conductor is a perfect reflector, so it can absorb and emit equal amounts of energy.

Hence, we can expect that the Poynting vector of the biconical antenna can emerge only from the feed point (at the tips of the cones) which is connected to the external power source. In this view, the antenna serves to guide the radiation away from its axis, but is not itself the primary source of the radiation.

The guiding occurs as the antenna conductors absorb and re-emit energy that emanates from the feed point. One could ask for a description of only the re-emitted energy without including the primary source. This appears to be the common approach in discussions of linear antennas [4], which leads to various ambiguities in the analysis (in this author's view). The present problem follows the lead of Schelkunoff in seeking an inclusive description of the flow of energy from the feed point outwards.

A conductor with finite conductivity can support a very small electric field parallel to its surface, and hence a Poynting vector perpendicular to the surface. However, the usual direction of the Poynting vector in "real" conductors is into the conductor, to provide the energy lost to Joule heating in the interior. See, for example, sec. 8.1 of [9].

Hence, we expect that the analysis below for a perfect conductor also gives a good approximation to the fields and Poynting vector in an antenna built with materials of large but finite conductivity.

The most novel feature of this note for those familiar with textbook discussion of dipole radiation may be the appearance of the "zero mode" (sec. 2.4.2) in the near zone of a linear antenna. In a sense, the conductors of the antenna form a kind of cavity or transmission line (for $r < a$) that has a fundamental mode which cannot propagate into free space.

## 2.1 A Wave Equation for the Vector Potential

We will work in a spherical coordinate system $(r, \theta, \phi)$ whose origin is at the common vertex of the two cones and whose $z$ axis coincides with that of the cones. The solution will be based on the use of potentials for the electromagnetic fields. The time-dependent currents $I(r, \theta_0, t)$ flow on the surface of the cones with no azimuthal variation, resulting in time-dependent accumulations of surface charge density $\sigma(r, \theta_0, t)$. Both the scalar potential $V$ and the vector potential $\mathbf{A}$ will be nontrivial. However, we can anticipate that the magnetic field lines will be purely transverse to the radial direction, $\mathbf{B} = B_\theta \hat{\boldsymbol{\theta}} + B_\phi \hat{\boldsymbol{\phi}}$ because the currents that generates the field are radial. Indeed, if the currents have no azimuthal variation, then we expect $B_\theta = 0$, but it is convenient to defer use of this insight until eq. (5).

Our first goal is a wave equation for the potentials $\mathbf{A}$ and $V$ for transverse magnetic (TM) waves in spherical coordinates.

The magnetic field has zero divergence,

$$0 = \boldsymbol{\nabla} \cdot \mathbf{B} = \frac{1}{r \sin\theta} \left( \frac{\partial (\sin\theta B_\theta)}{\partial \theta} + \frac{\partial B_\phi}{\partial \phi} \right), \tag{1}$$

so there is a scalar function $\Phi$ such that,

$$B_\theta = \frac{1}{r \sin\theta} \frac{\partial \Phi}{\partial \phi}, \qquad B_\phi = -\frac{1}{r} \frac{\partial \Phi}{\partial \theta}. \tag{2}$$

Since the magnetic field is also the curl of the vector potential, we can write,

$$\mathbf{B} = B_\theta \hat{\boldsymbol{\theta}} + B_\phi \hat{\boldsymbol{\phi}} = \boldsymbol{\nabla} \times \mathbf{A} = \frac{\hat{\boldsymbol{\theta}}}{r} \left( \frac{1}{\sin\theta} \frac{\partial A_r}{\partial \phi} - \frac{\partial (r A_\phi)}{\partial r} \right) + \frac{\hat{\boldsymbol{\phi}}}{r} \left( \frac{\partial (r A_\theta)}{\partial r} - \frac{\partial A_r}{\partial \theta} \right). \tag{3}$$

Comparison of eqs. (2) and (3) indicates that it suffices to consider the vector potential to be purely radial, with $A_r = \Phi$,

$$\mathbf{A} = A_r(\mathbf{r}, t) \hat{\mathbf{r}}. \tag{4}$$

Furthermore, we restrict our attention to waves of angular frequency $\omega$, and to the case that the source currents have no azimuthal dependence. Thus, we can write the vector potential as,

$$\mathbf{A}(\mathbf{r}, t) = A_r(r, \theta) e^{-i\omega t} \hat{\mathbf{r}}. \tag{5}$$

The usual strategy would be to deduce a wave equation for the vector potential by working in the Lorentz gauge, where the wave equations for the potentials take on a simple form.[2] However, the behavior of the Laplacian operator in spherical coordinates on a radial vector such as $A_r \hat{\mathbf{r}}$ mars the elegance of this approach.[3] Instead, we follow a procedure of Schelkunoff [7] that leads to a sufficiently simple version of a wave equation (strictly, a Helmholtz equation) without explicit statement of the gauge condition.

We first note that the components of the magnetic field due to the vector potential (5) are,

$$B_r = 0, \qquad B_\theta = 0, \qquad B_\phi = -\frac{1}{r} \frac{\partial A_r}{\partial \theta}. \tag{9}$$

The electric field is obtained from the potentials according to,

$$\mathbf{E} = -\boldsymbol{\nabla} V - \frac{1}{c} \frac{\partial \mathbf{A}}{\partial t}, \tag{10}$$

where the scalar potential $V$ is also independent of azimuth, and is taken to have oscillatory time dependence,

$$V(\mathbf{r}, t) = V(r, \theta) e^{-i\omega t}. \tag{11}$$

---

[2] When the potentials obey the Lorentz gauge condition (in Gaussian units),

$$\boldsymbol{\nabla} \cdot \mathbf{A} = -\frac{1}{c} \frac{\partial V}{\partial t}, \tag{6}$$

the free-space wave equation for the vector potential is,

$$\nabla^2 \mathbf{A} = \frac{1}{c^2} \frac{\partial^2 \mathbf{A}}{\partial t^2}. \tag{7}$$

[3] From p. 116 of [10] we find that for the vector potential (5),

$$\nabla^2 (A_r \hat{\mathbf{r}}) = \hat{\mathbf{r}} \left( \nabla^2 A_r - \frac{2 A_r}{r^2} \right) - \hat{\boldsymbol{\theta}} \frac{2}{r^2} \frac{\partial A_r}{\partial \theta}. \tag{8}$$

The components of the electric field are then,

$$E_r = -\frac{\partial V}{\partial r} + ikA_r, \qquad E_\theta = -\frac{1}{r}\frac{\partial V}{\partial \theta}, \qquad E_\phi = 0, \tag{12}$$

where we have introduced the wave number $k = \omega/c$.

Additional relations between the components of the electric and magnetic fields can be found from the fourth Maxwell equation, which in free space is,

$$\boldsymbol{\nabla} \times \mathbf{B} = \frac{1}{c}\frac{\partial \mathbf{E}}{\partial t} = -ik\mathbf{E}. \tag{13}$$

The $r$ and $\theta$ components of eq. (13) tells us that,

$$-ikE_r = \frac{1}{r\sin\theta}\frac{\partial(\sin\theta B_\phi)}{\partial\theta} = -\frac{1}{r^2\sin\theta}\frac{\partial}{\partial\theta}\left(\sin\theta\frac{\partial A_r}{\partial\theta}\right) = -\frac{1}{r^2}\frac{\partial^2[(1-\cos^2\theta)A_r]}{\partial(\cos\theta)^2}, \tag{14}$$

$$-ikE_\theta = -\frac{1}{r}\frac{\partial(rB_\phi)}{\partial r} = \frac{1}{r}\frac{\partial^2 A_r}{\partial r\partial\theta}, \tag{15}$$

using eq. (9). Substituting eq. (12) into eq. (15) we can integrate once to find

$$\frac{\partial A_r}{\partial r} = ikV. \tag{16}$$

This is, in effect, the gauge condition for this problem, which differs from the Lorentz condition (6).

Inserting relation (16) into the expression (12) for $E_r$ we now have,

$$E_r = \frac{i}{k}\frac{\partial^2 A_r}{\partial r^2} + ikA_r. \tag{17}$$

Combining this with eq. (14) we find at last the desired Helmholtz equation for scalar $A_r$, from which the electromagnetic fields can be deduced,

$$\frac{\partial^2 A_r}{\partial r^2} + \frac{1}{r^2}\frac{\partial^2[(1-\cos^2\theta)A_r]}{\partial(\cos\theta)^2} + k^2A_r = 0. \tag{18}$$

## 2.2 Series Expansion of the Vector Potential

We seek a solution of the Helmholtz equation (18) that is a sum of terms of the form,

$$A_r(r,\theta) = R(r)\Theta(\theta). \tag{19}$$

We insert the trial solution (19) into eq. (18), multiply by $r^2$ and divide by $A_r$ to find

$$r^2\frac{d^2R}{dr^2} + k^2r^2 + \frac{1}{\Theta}\frac{d^2}{d(\cos\theta)^2}[(1-\cos^2\theta)\Theta] = 0. \tag{20}$$

As is usual for separation-of-variables techniques in spherical coordinates, we introduce a separation constant $\pm n(n+1)$ to obtain the radial and polar equations

$$\frac{d^2R_n}{d(kr)^2} + \left[1 - \frac{n(n+1)}{(kr)^2}\right]R_n = 0, \tag{21}$$

$$\frac{d^2}{d(\cos\theta)^2}[(1-\cos^2\theta)\Theta_n] + n(n+1)\Theta_n = 0. \tag{22}$$

Solutions to polar eq. (15) are the familiar Legendre functions,

$$\Theta_n = P_n(\cos\theta). \tag{23}$$

The Legendre functions $P_n$ can be defined for any $n$ real or complex (see, for example, sec. 3.6 of [7] or chap. 8 of [11]), but when the angular region of interest is $0 \le \theta \le \pi$ the separation constant $n$ must be an integer so that $P_n(\pm 1)$ is finite.

We will first consider solutions over the full angular range $0 \le \theta \le \pi$ (sec. 2.3), before turning to the problem of the biconical antenna (sec. 2.4) in which $\theta_0 \le \theta \le \pi - \theta_0$ for $r < a$.

The polar equation eq. (15) is also solved by the Legendre functions $Q_n$, which diverge at $\theta = 0$ and $\pi$. Hence, we will not use these functions when considering the entire angular region $0 \le \theta \le \pi$. As will be shown in sec. 2.4, it also suffices to use only the $P_n$ even on the restricted angular interval $\theta_0 \le \theta \le \pi - \theta_0$.

The three lowest-order $P_n$ for integer $n$ are,

$$P_0(\cos\theta) = 1, \quad P_1(\cos\theta) = \cos\theta, \quad P_2(\cos\theta) = \frac{3\cos^2\theta - 1}{2}\,. \tag{24}$$

The radial equation (21) is sometimes called the Riccati-Bessel equation, whose solutions are $kr$ times the so-called spherical Bessel functions of order $n$. The latter are related to ordinary Bessel functions of order $n + \frac{1}{2}$ (see, for example, secs. 5.31 and 5.37 of [8], sec. 10.1 of [11], sec. 9.6 of [9]). At large $r$, we expect the electromagnetic fields to consist of spherical waves of the form $e^{i(kr-\omega t)}/r$. As seen above, these fields have the form of $1/r$ times derivatives of the vector potential $A_r$. This suggests that we use ($kr$ times) spherical Bessel functions of the third kind,

$$h_n^{(1)}(kr) = j_n(kr) + i y_n(kr), \tag{25}$$

where $j_n$ and $y_n$ are the spherical Bessel functions of the first and second kind, as the asymptotic is behavior of $h_n^{(1)}$ is

$$h_n^{(1)}(kr \gg 1)) \to (-i)^{n+1}\frac{e^{ikr}}{kr}\,. \tag{26}$$

The three lowest-order $h_n^{(1)}$ are,

$$h_0^{(1)}(kr) = -i\frac{e^{ikr}}{kr}\,, \quad h_1^{(1)}(kr) = -\frac{e^{ikr}}{kr}\left(1 + \frac{i}{kr}\right), \quad h_2^{(1)}(kr) = i\frac{e^{ikr}}{kr}\left(1 + \frac{3i}{kr} - \frac{3}{(kr)^2}\right). \tag{27}$$

Altogether, our expansion for the vector potential is,

$$A_r(r,\theta,t) = kr\sum_{n=0}^{\infty} A_n h_n^{(1)}(kr) P_n(\cos\theta) e^{-i\omega t}, \tag{28}$$

where the $A_n$ are Fourier coefficients to be determined.

We also note that eqs. (17) and (21) can be combined to give a simpler expression for the radial component of the $n$th term of the expansion for the electric field:

$$E_{r,n} = \frac{in(n+1)A_{r,n}}{kr^2}\,. \tag{29}$$

## 2.3 TM Fields from Point Sources

The expansion (28), when applied for all polar angles $0 \le \theta \le \pi$, represents the radiation of a series of oscillating ideal (point) electric multipoles, for which the waves have transverse magnetic (TM) fields.

The electromagnetic fields can be calculated from eq. (28) using eqs. (9), (14) and (15), all of which involve the derivative $\partial A_r/\partial\theta$. For this, we note that,

$$\frac{dP_n}{d\theta} = \frac{n}{\sin\theta}\left(\cos\theta P_n - P_{n-1}\right). \tag{30}$$

Hence, there is no contribution to the electromagnetic fields from the $n = 0$ (monopole) term, and the lowest order multipole of significance is, as expected, the $n = 1$ (dipole) term.

The $n = 1$ (electric dipole) potential is, referring to eq. (27),

$$A_r^{E1} = -A_1 e^{i(kr-\omega t)}\left(1 + \frac{i}{kr}\right)\cos\theta, \qquad \frac{\partial A_r^{E1}}{\partial\theta} = A_1 e^{i(kr-\omega t)}\left(1 + \frac{i}{kr}\right)\sin\theta. \tag{31}$$

The dipole electromagnetic fields are (we can also use eq. (29) to obtain $E_r$),

$$E_r^{E1} = -2iA_1\frac{e^{i(kr-\omega t)}}{kr^2}\left(1 + \frac{i}{kr}\right)\cos\theta, \tag{32}$$

$$E_\theta^{E1} = -A_1\frac{e^{i(kr-\omega t)}}{r}\left(1 + \frac{i}{kr} - \frac{1}{k^2r^2}\right)\sin\theta, \tag{33}$$

$$E_\phi^{E1} = B_r^{E1} = B_\theta^{E1} = 0,$$

$$B_\phi^{E1} = -A_1\frac{e^{i(kr-\omega t)}}{r}\left(1 + \frac{i}{kr}\right)\sin\theta. \tag{34}$$

These forms agree with the standard results (see, for example, sec. 9.2 of [9]) with the identification that $A_1 = -k^2 p$ where $p$ is the peak electric dipole moment of the source.

Similarly, the $n = 2$ (axially symmetric electric quadrupole) fields are,

$$A_r^{E2} = iA_2 e^{i(kr-\omega t)}\left(1 + \frac{3i}{kr} - \frac{3}{(kr)^2}\right)\frac{3\cos^2\theta - 1}{2}, \tag{35}$$

$$\frac{\partial A_r^{E2}}{\partial\theta} = -3iA_2 e^{i(kr-\omega t)}\left(1 + \frac{3i}{kr} - \frac{3}{(kr)^2}\right)\sin\theta\cos\theta. \tag{36}$$

$$E_r^{E2} = -3A_2\frac{e^{i(kr-\omega t)}}{kr^2}\left(1 + \frac{3i}{kr} - \frac{3}{(kr)^2}\right)(3\cos^2\theta - 1), \tag{37}$$

$$E_\theta^{E2} = 3iA_2\frac{e^{i(kr-\omega t)}}{r}\left(1 + \frac{3i}{kr} - \frac{6}{k^2r^2} - \frac{6i}{k^3r^3}\right)\sin\theta\cos\theta, \tag{38}$$

$$E_\phi^{E2} = B_r^{E2} = B_\theta^{E2} = 0,$$

$$B_\phi^{E2} = 3iA_2\frac{e^{i(kr-\omega t)}}{r}\left(1 + \frac{3i}{kr} - \frac{3}{(kr)^2}\right)\sin\theta\cos\theta. \tag{39}$$

Sketches of the electric field lines for the time-dependent electric dipole and electric quadrupole are shown below (from [7]). The original paper on electric dipole radiation by

Hertz [1] has an excellent "animation" showing the development of the near field during one cycle of the oscillation of the source.

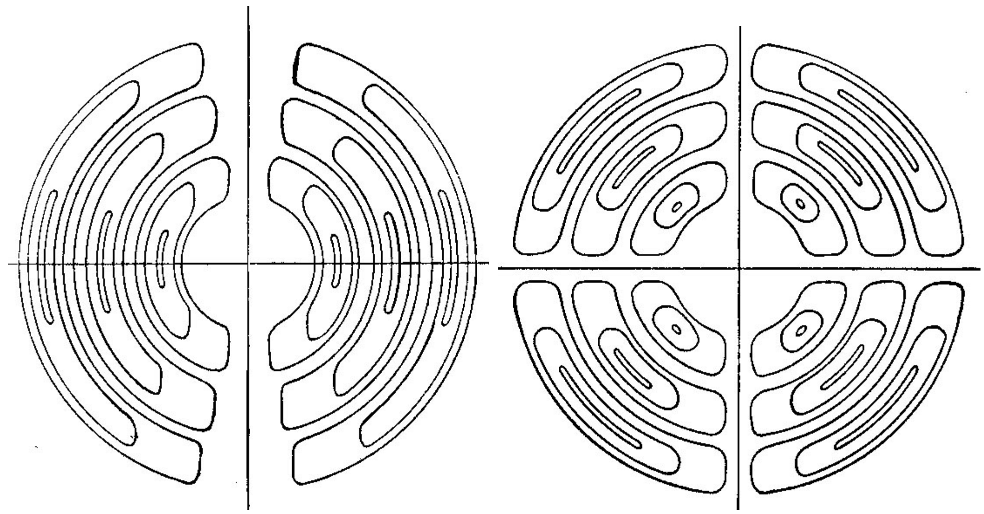

The flow of electromagnetic energy is described by the Poynting vector,

$$\mathbf{S} = \frac{c}{4\pi}\mathbf{E} \times \mathbf{B} = \frac{c}{4\pi}(\hat{\mathbf{r}}E_\theta B_\phi - \hat{\boldsymbol{\theta}}E_r B_\phi). \tag{40}$$

The time-average energy flow is given by,

$$\langle \mathbf{S} \rangle = \frac{c}{8\pi} Re(\mathbf{E}^\star \times \mathbf{B}) = \frac{c}{8\pi} Re(\hat{\mathbf{r}}E_\theta^\star B_\phi - \hat{\boldsymbol{\theta}}E_r^\star B_\phi). \tag{41}$$

For the dipole fields (32)-(34) we find,

$$\left\langle \mathbf{S}^{E1} \right\rangle = \hat{\mathbf{r}}\frac{cA_1^2}{8\pi r^2}\sin^2\theta, \tag{42}$$

and for the quadrupole fields (37)-(39) we have,

$$\left\langle \mathbf{S}^{E2} \right\rangle = \hat{\mathbf{r}}\frac{cA_2^2}{8\pi r^2}\sin^2\theta\cos^2\theta. \tag{43}$$

The time-average energy flow is purely radial and falls off as $1/r^2$ at any distance from the point source. This is consistent with conservation of energy which is radiated from the point source. Hence, we can say that the time-average Poynting vectors (40) and (41) describe radiation both in the near and far zones [2].

The forms of the electromagnetic fields that we have discussed thus far have all been transverse magnetic (TM), which we have identified with electric multipoles. For any set of fields $\mathbf{E}$ and $\mathbf{B}$, the dual fields $\mathbf{E}' = -\mathbf{B}$ and $\mathbf{B}' = -\mathbf{E}$ are also solutions to Maxwell's equations in free space. Hence, the present formalism can be transformed to describe a family of transverse electric (TE) fields, which we identify with magnetic multipoles.

## 2.4 Fields of a Biconical Antenna

The field patterns of the electric multipoles found in the previous section all vanish along the $z$ axis. Hence, we may expect that those field patterns would be only slightly perturbed if a pair of conductors were placed along the $z$ axis, one for $z > 0$ and the other for $z < 0$, either as two thin wires or even as a pair of cones of half angle $\theta_0$. Since a perfect conductor can only support electric fields that are perpendicular to its surface, we anticipate that the field patterns in the presence of the conductors will include half loops of field lines that emerge from the conductors and rejoin them less than half a wavelength away. The figures below sketch this possibility for the case of electric dipole and electric quadrupole field patterns.

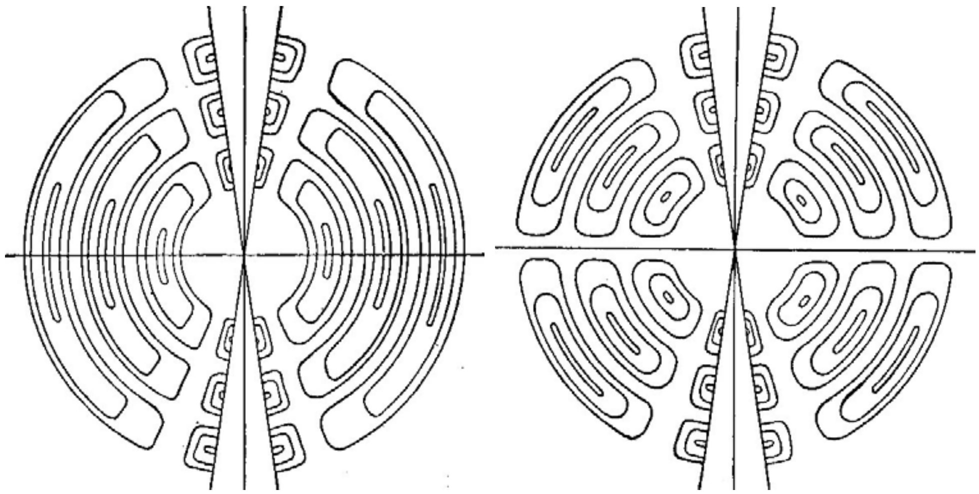

The field lines that are attached to the conductors would travel outwards along the conductors (if the latter are long enough) in a manner reminiscent of wave propagation close to a wire (see, for example, p. 535 of [12]). Indeed, if the conductors are extremely long, it would be more appropriate to call this a transmission line problem than an antenna problem.

Here, we will consider examples where the length $a$ of the axis of the cones is less than a wavelength. If the half angle $\theta_0$ of the cones (shown on p.1) is small, we may suppose that the fields patterns found in the previous section hold to a good approximation for $r > a$. The fields in the region $r < a$ will, to a good approximation, be the same as the fields in this region if the conical conductors were infinitely long.

### 2.4.1 Expansion of the Vector Potential

We seek the appropriate modifications of the fields found in sec. 2.3 supposing the region of interest $\theta_0 \le \theta \le \pi - \theta_0$ is bounded by perfect conductors. The tangential electric field must vanish on these conductor, *i.e.*, $E_r(r, \theta_0) = E_r(r, \pi - \theta_0) = 0$. recalling eq. (14), this boundary condition will be satisfied by requiring,

$$A_r(r, \theta_0) = A_r(r, \pi - \theta_0) = 0. \tag{44}$$

Again writing $A_r(r, \theta) = R_n(r)\Theta_n(\theta)$, the Legendre functions $P_n$ are suitable forms for the angular functions $\Theta_n$. However, since the $z$-axis is excluded from the region of interest, the index $n$ need not be an integer. We will find that for small cone angles $\theta_0$, the indices $n$ differ only slightly from unity. Legendre functions with indices close to an integer (*i.e.*, $n = m + \Delta$ where $m$ is an integer and $|\Delta| \ll 1$) obey (see p. 58 of [7]),

$$P_{m+\Delta}(\cos\theta) \approx P_m(\cos\theta) \left[1 + 2\Delta \ln \cos\frac{\theta}{2}\right]. \tag{45}$$

This expression is poorly behaved as $\theta \to \pi$, so it is useful to note an additional relation that is well-behaved at $\theta = \pi$ but poorly behaved at $\theta = 0$,

$$P_{m+\Delta}(-\cos\theta) \approx (-1)^m P_m(\cos\theta)\left[1 + 2\Delta \ln\sin\frac{\theta}{2}\right]. \tag{46}$$

The figure below shows $P_{m+\Delta}(-\cos\theta)$ for $m = 0$ and 1 and $\Delta = 0$, 0.1 and 0.2 (from [7]).

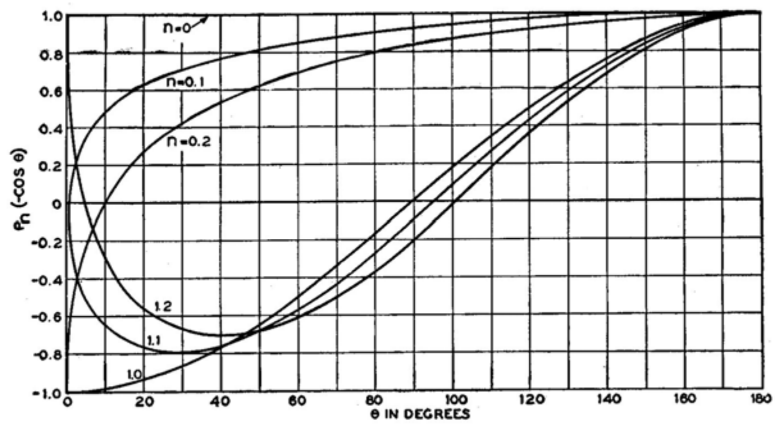


We can regard the $P_{m+\Delta}(\cos\theta)$ and the $P_{m+\Delta}(-\cos\theta)$ as separate sets of functions, and use combinations of them in our solution. The condition (44) can be satisfied by the form,

$$\Theta_n(\theta) = \frac{1}{2}[P_n(\cos\theta) - P_n(-\cos\theta)], \tag{47}$$

provided

$$P_n(\cos\theta_0) = P_n(-\cos\theta_0), \tag{48}$$

or by,

$$\Theta_n(\theta) = \frac{1}{2}[P_n(\cos\theta) + P_n(-\cos\theta)], \tag{49}$$

provided,

$$P_n(\cos\theta_0) = -P_n(-\cos\theta_0). \tag{50}$$

If index $n$ were an integer, eq. (48) would imply that $n$ is even, and eq. (50) would imply that $n$ is odd, but then eqs. (47) and (49) would yield $\Theta_n = 0$. However, the form of the Legendre functions when $n$ is not an integer is such that eqs. (47)-(50) can be satisfied in a nontrivial manner.

We restrict our attention to cones with small angle $\theta_0$. Then, according to eq. (45), $P_n(\cos\theta_0) \approx 1$ for any $n$. To satisfy eqs. (48) and (50) we need $P_n(-\cos\theta_0) \approx \pm 1$. From eq. (46), for $\theta = \pi - \theta_0$ with $\theta_0$ small, we see that $P_{m+\Delta}(-\cos\theta_0) \approx (-1)^m P_{m+\Delta}(\cos\theta_0) \approx (-1)^m$ provided,

$$\Delta = -\frac{1}{\ln\sin\frac{\theta_0}{2}} \approx -\frac{1}{\ln\frac{\theta_0}{2}} = \frac{1}{\ln\frac{2}{\theta_0}} \ll 1, \tag{51}$$

where $m$ is an integer. Thus, the angular functions $\Theta_n$ of both forms (47) and (49) are given by,

$$\Theta_{m+\Delta}(\theta) \approx \left(1 + \Delta \ln\frac{\sin\theta}{2}\right) P_m(\cos\theta), \tag{52}$$

where $m$ is an integer and $\Delta$ is given by eq. (51). Note that $\Theta_{m+\Delta}(\theta_0) = \Theta_{m+\Delta}(\pi - \theta_0) = 0$ for small $\theta_0$. The figures below show $\Theta_\Delta$ and $\Theta_{1+\Delta}$ (from [7]).

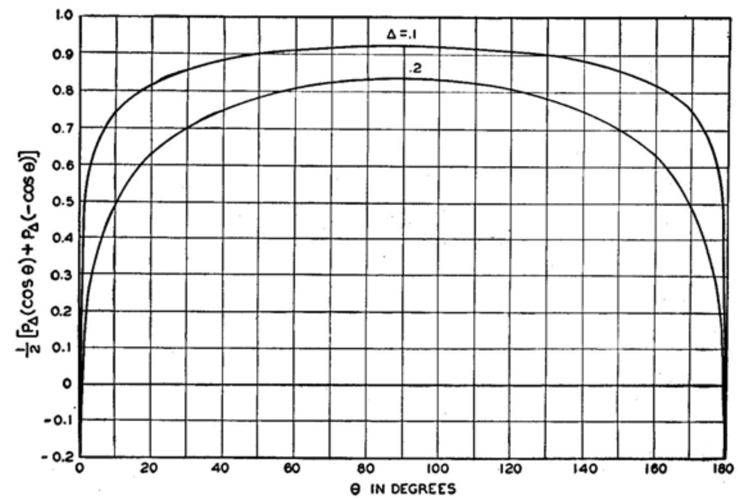


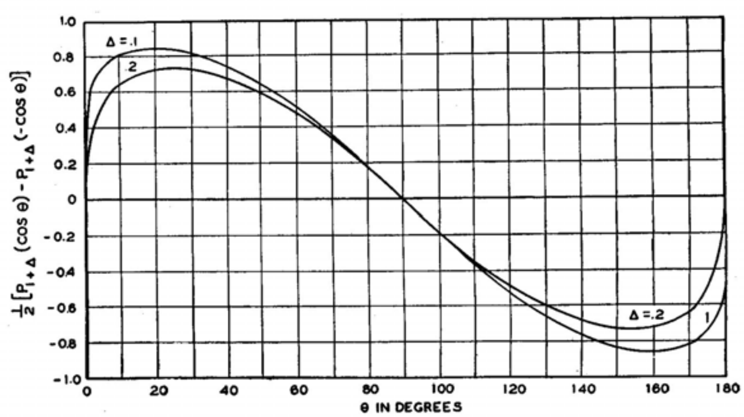


Turning now to the radial functions $R_n(r)$, from the analysis of sec. 2.3 these can be written as,

$$R_n(r) = krh^{(1)}_{m+\Delta}(kr). \tag{53}$$

For small $\Delta$, $h^{(1)}_{m+\Delta}(kr)$ is well approximated by $h^{(1)}_m(kr)$. This can be inferred, for example, from Sonine's integral (eq. (11.4.10) of [11]).

Thus, a suitable expansion for the vector potential in the region $\theta_0 \leq \theta \leq \pi - \theta_0$, when bounded by perfect conductors, is,

$$A_r(r, \theta, t) = \sum_{n=0}^{\infty} A_{r,n}(r, \theta, t) = kr\left(1 + \Delta \ln \frac{\sin\theta}{2}\right) B_n h^{(1)}_n(kr) P_n(\cos\theta) e^{-i\omega t}, \tag{54}$$

where the $B_n$ are Fourier coefficients to be determined. As expected, this expansion is very similar to that for a series of point electric multipoles that radiate into the entire region $0 \leq \theta \leq \pi$.

We note some of the symmetries of the electromagnetic fields of the modes of index $n$ in the expansion (54). In view of the definitions (47) and (49), the term $A_{r,n}$ in the expansion of the vector potential obeys,

$$A_{r,n}(r,\pi-\theta,t) = (-1)^n A_{r,n}(r,\theta,t), \qquad \frac{\partial A_{r,n}(r,\pi-\theta,t)}{\partial\theta} = (-1)^{n+1}\frac{\partial A_{r,n}(r,\theta,t)}{\partial\theta}. \tag{55}$$

According to eq. (29), the radial component of the electric field of the $n^{\text{th}}$ mode is proportional to the vector potential, $E_{r,n} = in(n+1)A_{r,n}/kr^2$. Hence,

$$E_{r,n}(r,\pi-\theta,t) = (-1)^n E_{r,n}(r,\theta,t). \tag{56}$$

Similarly, the $\theta$ component of the electric field and the $\phi$ component of the magnetic field are proportional to $\partial A_r/\partial\theta$ (or its radial derivative), so we have,

$$E_{\theta,n}(r,\pi-\theta,t) = (-1)^{n+1}E_{\theta,n}(r,\theta,t), \qquad B_{\phi,n}(r,\pi-\theta,t) = (-1)^{n+1}B_{\phi,n}(r,\theta,t). \tag{57}$$

The latter relation tells us that the magnetic field circulates about the $z$-axis in the same sense for both cones for odd-$n$ modes, but in the opposite sense for the two cones for even-$n$ modes. Then, by Ampère's law, the radial currents that drive these modes are in the same direction (along a generator of the cones) for both cones in odd-$n$ modes, but in the opposite direction for even-$n$ modes.

This problem concerns a center-fed biconical antenna, which implies that the currents must be in the same direction along a generator of the two cones (since the currents in the two conductors of the feed line are in opposite directions, so that a positive current in the line attached to the "upper" cone leads to an "upward" current in that cone while a negative current in the line attached to the "lower" cone leads to an "upward" current in that cone as well). Hence, we infer that only odd-$n$ modes are excited in a center-fed antenna.

However, as we show below, our approximations have not been sufficiently precise for a good description of the zero mode, which proves to be strongly excited for a center-fed biconical antenna.

### 2.4.2 The TEM Zero Mode

An important difference between the vector potential (54) and that of eq. (28) is that the former supports a nontrivial mode when $n = 0$. Using eqs. (9), (15) and (29), we find,

$$\begin{aligned}
A_r^0(r,\theta,t) &= -iB_0\left(1+\Delta\ln\frac{\sin\theta}{2}\right)e^{i(kr-\omega t)}, && (58)\\
\frac{\partial A_r^0}{\partial\theta} &= -iB_0\Delta\cot\theta e^{i(kr-\omega t)}, && (59)\\
E_r^0 &= 0, && (60)\\
E_\theta^0 &= iB_0\Delta\cot\theta\frac{e^{i(kr-\omega t)}}{r}, && (61)\\
E_\phi^0 = B_r^0 = B_\theta^0 &= 0, && (62)\\
B_\phi^0 &= iB_0\Delta\cot\theta\frac{e^{i(kr-\omega t)}}{r}. && (63)
\end{aligned}$$

The electric field lines are purely azimuthal, as shown in the figure below. This is a transverse electric and magnetic (TEM) mode. The lines at a given value of $r$ all converge onto, or emanate from, the conical surface where they are terminated/created by surface charges. Hence, this mode cannot exist in the absence of a conductor, and was absent in the modes found in sec. 2.3.

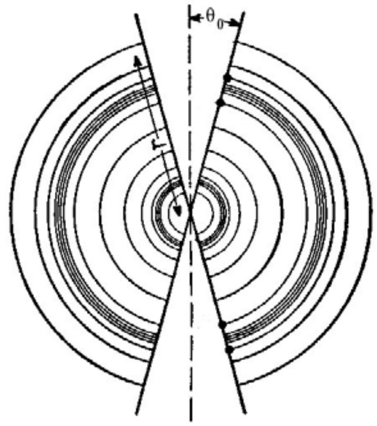


Although we have identified the existence of an $n = 0$ mode via our approximate vector potential (54), the details represented in eqs. (58)-(63) are not quite correct. A formal clue is that in free space we should have $\boldsymbol{\nabla} \cdot \mathbf{E} = 0$, but according to eq. (62),

$$\boldsymbol{\nabla} \cdot \mathbf{E}^0 = \frac{1}{r \sin\theta} \frac{\partial(\sin\theta E_\theta^0)}{\partial\theta} = -iB_0\Delta \cos\theta \frac{e^{i(kr-\omega t)}}{r} \neq 0. \tag{64}$$

Apparently the angular dependence of $E_\theta^0$ must be $1/\sin\theta$, not $\cot\theta$ if this is to be the only nonzero component of the electric field.

Another clue that our characterization of the zero mode is not quite correct is obtained by calculating the voltage difference $V_0$ between a point a radius $r$ on one cone and a corresponding point on the other. Recalling eqs. (15) and (44), this is,

$$V_0(r,t) = \int_{\theta_0}^{\pi-\theta_0} E_\theta^0 \, r d\theta = \frac{i}{k} \int_{\theta_0}^{\pi-\theta_0} \frac{\partial^2 A_r^0}{\partial r \partial\theta} d\theta = \frac{i}{k} \left( \frac{\partial A_r^0(r, \pi - \theta_0)}{\partial r} - \frac{\partial A_r^0(r, \theta_0)}{\partial r} \right) e^{i(kr-\omega t)} = 0, \tag{65}$$

Indeed, this calculation shows that the voltage difference $V_n(r,t)$ vanishes for every term $n$ of the expansion (54). But it is unphysical that the currents on the cones can arise without any voltage differences over the cones. A nonzero voltage must arise for at least one mode, which we now anticipate to be the zero mode.

To understand what we have overlooked, we return to the separated equation (22) for the angular function $\Theta(\theta)$ and re-examine the case when $n = 0$. Then, we have,

$$0 = \frac{d^2[(1 - \cos^2\theta)\Theta]}{d(\cos\theta)^2} = \frac{1}{\sin\theta} \frac{d}{d\theta} \left( \sin\theta \frac{d\Theta}{d\theta} \right). \tag{66}$$

In addition to the solution $\Theta_0 = 1 = P_0$ that we previously assumed, we also can have the solution,

$$\Theta_0 = 1 + \Delta \ln \tan \frac{\theta}{2}. \tag{67}$$

For small $\theta$ this is equivalent to $1 + \Delta \ln \sin(\theta/2)$, which is quite close to eq. (58).

Note that the zero-mode angular function (67) corresponds to an exact solution of the Helmholtz equation (18) for zero separation constant (which solution can be physical only if the $z$ axis is excluded from the region of interest). In contrast, our approximate solution (58) corresponds to a small but nonzero separation constant $\Delta(\Delta+1)$.

Using the form (67) for $\Theta_0$, the fields of the zero mode can be written as,

$$A_r^0(r,\theta,t) = -iB_0\left(1+\Delta\ln\tan\frac{\theta}{2}\right)e^{i(kr-\omega t)}, \tag{68}$$

$$\frac{\partial A_r^0}{\partial\theta} = -\frac{iB_0\Delta}{\sin\theta}e^{i(kr-\omega t)}, \tag{69}$$

$$E_r^0 = 0, \tag{70}$$

$$E_\theta^0 = \frac{iB_0\Delta}{\sin\theta}\frac{e^{i(kr-\omega t)}}{r}, \tag{71}$$

$$E_\phi^0 = B_r^1 = B_\theta^0 = 0, \tag{72}$$

$$B_\phi^0 = \frac{iB_0\Delta}{\sin\theta}\frac{e^{i(kr-\omega t)}}{r}. \tag{73}$$

Inserting eq. (68) into eq. (65), the voltage at radius $r$ in the zero mode is,

$$\begin{aligned} V_0(r,t) &= -2iB_0\Delta\ln\tan\frac{\theta_0}{2}e^{i(kr-\omega t)} = 2iB_0\Delta\ln\frac{1+\cos\theta_0}{\sin\theta_0}e^{i(kr-\omega t)} \\ &\approx 2iB_0\Delta\ln\frac{2}{\theta_0}e^{i(kr-\omega t)} = 2iB_0e^{i(kr-\omega t)}. \end{aligned} \tag{74}$$

Thus, we can relate the coefficient $iB_0$ that described the strength of the zero mode to the peak voltage $V_0(0)$ that is applied across the tips of the cones,

$$iB_0 = \frac{V_0(0)}{2}. \tag{75}$$

The radial current $I_0$ on the surface of the cone follows from Ampère's law as,

$$I_0(r,t) = \frac{cr\sin\theta_0 B_\phi^0(r,\theta_0,t)}{2} = \frac{icB_0\Delta}{2}e^{i(kr-\omega t)} \equiv I_0(0)e^{i(kr-\omega t)}. \tag{76}$$

Thus, the voltage and current at radius $r$ are related by,

$$V_0(r,t) = \frac{4}{c}\ln\frac{2}{\theta_0}I_0(r,t) = \frac{4}{c\Delta}I_0(r,t) \equiv Z_0(r)I_0(r,t), \tag{77}$$

where,

$$Z_0(r) = \frac{4}{c\Delta} = \frac{120\Omega}{\Delta} = 120\Omega\ \ln\frac{2}{\theta_0} \tag{78}$$

is the (transmission line) impedance of the zero mode, which is independent of position. Recall that $1/c = 30\Omega$ in Gaussian units.

The surface charge density $\sigma_0$ at distance $r$ from the apex of the cones is given by,

$$\sigma_0(r,t) = \frac{E_\theta^0(r,\theta_0,t)}{4\pi} = \frac{iB_0\Delta}{4\pi\sin\theta_0}\frac{e^{i(kr-\omega t)}}{r} = \frac{I_0(0)}{2\pi c\sin\theta_0}\frac{e^{i(kr-\omega t)}}{r}. \tag{79}$$

This is large at the tip of the cone, as is to be expected.

The Poynting vector for the zero mode is purely radial and falls off as $1/r^2$,

$$\mathbf{S} = \frac{c}{4\pi}\hat{\mathbf{r}} Re(E_\theta) Re(B_\phi) = \frac{I_0^2(0)}{\pi c \sin^2\theta} \frac{\cos^2(kr - \omega t)}{r^2}. \tag{80}$$

The flow of energy is from the feed point at the origin into the surrounding space outside the two cones. The energy flow is highest close to the surface of the cones.[4]

The time-average power emitted into the zero mode is,

$$\langle P \rangle = \int r^2 \langle S_r \rangle \, d\Omega = \frac{I_0^2(0)}{\pi c} \frac{1}{2} 4\pi \int_{\theta_0}^{\pi/2} \frac{d \sin\theta}{\sin\theta} = \frac{1}{2}\frac{4}{c} \ln \frac{1}{\sin\theta_0} I_0^2(0) \approx \frac{1}{2} Z_0 I_0^2(0). \tag{81}$$

If we think of the fields of the zero mode as a kind of radiation, rather than as the fields of a transmission line, then $Z_0$ can also be interpreted as the radiation resistance of this mode.

### 2.4.3 The Dipole-like Mode

The dipole-like mode ($n = 1$) is,

$$A_r^1(r,\theta,t) = -B_1 \left(1 + \Delta \ln \frac{\sin\theta}{2}\right) \cos\theta e^{i(kr-\omega t)} \left(1 + \frac{i}{kr}\right), \tag{82}$$

$$\frac{\partial A_r^0}{\partial\theta} = B_1 \left(1 + \Delta \ln \frac{\sin\theta}{2} - \Delta \cot^2\theta\right) \sin\theta e^{i(kr-\omega t)} \left(1 + \frac{i}{kr}\right), \tag{83}$$

$$E_r^1 = -2iB_1 \left(1 + \Delta \ln \frac{\sin\theta}{2}\right) \cos\theta \frac{e^{i(kr-\omega t)}}{kr^2} \left(1 + \frac{i}{kr}\right), \tag{84}$$

$$E_\theta^1 = -B_1 \left(1 + \Delta \ln \frac{\sin\theta}{2} - \Delta \cot^2\theta\right) \sin\theta \frac{e^{i(kr-\omega t)}}{r} \left(1 + \frac{i}{kr} - \frac{1}{k^2 r^2}\right), \tag{85}$$

$$E_\phi^1 = B_r^1 = B_\theta^1 = 0, \tag{86}$$

$$B_\phi^1 = -B_1 \left(1 + \Delta \ln \frac{\sin\theta}{2} - \Delta \cot^2\theta\right) \sin\theta \frac{e^{i(kr-\omega t)}}{r} \left(1 + \frac{i}{kr}\right). \tag{87}$$

### 2.4.4 Fields of a Short Center-Fed Biconical Antenna

For a short antenna, we expect the fields for $r < a$ to be well described by a combination of the zero mode, eqs. (70)-(73) where $iB_0 = V_0(0)/2$, and the dipole-like mode, eqs. (84)-(87). For $r > a$, the fields are to a good approximation the free-space dipole fields, eqs. (32)-(34).

The Fourier coefficients $A_1$ and $B_1$ are chosen so that the fields will be continuous at $r = a$. Thus, setting $A_1 = B_1$ insures continuity of $E_r$ to within an "error" of $\Delta \ln 2$. To have $E_\theta$ and $B_\phi$ continuous across $r = a$, the $1/\sin\theta$ dependence seen for these components in the zero mode, but not in the free-space dipole mode, must be canceled as well as possible by the dipole-like mode for $r < a$. The largest part of eq. (85) that varies as $1/\sin\theta$ at $r = a$ is, for $ka \ll 1$,

$$- B_1 \Delta \frac{\cos^2\theta}{\sin\theta} \frac{e^{i(ka-\omega t)}}{k^2 a^3}. \tag{88}$$

[4] Compare with the figures on p. 15 of [4] for linear dipole antennas.

We therefore set $B_1 = V_0(0)(ka)^2/2$, which insures continuity of $E_\theta$ and $B_\phi$ to accuracy $\Delta(1 + \ln 2)$.

The fields for $r < a$ and $\theta_0 < \theta < \pi - \theta_0$ for a short ($ka \ll 1$), center-fed biconical antenna subject to peak voltage $V_0(0)$ across the feed points is, to accuracy $\Delta = 1/\ln(\theta_0/2)$ where $\theta_0 \ll 1$ is the cone angle,

$$E_r(r < a, \theta, t) = -iV_0(0)(ka)^2 \left(1 + \Delta \ln \frac{\sin\theta}{2}\right) \cos\theta \frac{e^{i(kr-\omega t)}}{kr^2} \left(1 + \frac{i}{kr}\right), \tag{89}$$

$$E_\theta(r < a, \theta, t) = \frac{V_0(0)}{2} \sin\theta \frac{e^{i(kr-\omega t)}}{r} \left\{\frac{\Delta}{\sin^2\theta} - (ka)^2 \left(1 + \Delta \ln \frac{\sin\theta}{2} - \Delta \cot^2\theta\right) \left(1 + \frac{i}{kr} - \frac{1}{k^2 r^2}\right)\right\}, \tag{90}$$

$$E_\phi = B_r = B_\theta = 0, \tag{91}$$

$$B_\phi(r < a, \theta, t) = \frac{V_0(0)}{2} \sin\theta \frac{e^{i(kr-\omega t)}}{r} \left\{\frac{\Delta}{\sin^2\theta} - (ka)^2 \left(1 + \Delta \ln \frac{\sin\theta}{2} - \Delta \cot^2\theta\right) \left(1 + \frac{i}{kr}\right)\right\}. \tag{92}$$

The fields for $r > a$ are, to similar accuracy, given by eqs. (90)-(92) on setting $\Delta$ to zero.

The time-average Poynting vector for $r < a$ is purely radial. To accuracy $\Delta$ we find,

$$\begin{aligned} \langle \mathbf{S} \rangle &= \frac{c}{8\pi} Re(\mathbf{E}^\star \times \mathbf{B}) = \frac{c\hat{\mathbf{r}}}{8\pi} Re(E_\theta^\star B_\phi) \\ &= \frac{c\hat{\mathbf{r}} V_0^2(0)}{32\pi} \frac{\sin^2\theta}{r^2} \left[(ka)^4 \left(1 + 2\Delta \ln \frac{\sin\theta}{2} - 2\Delta \cot^2\theta\right) + \frac{\Delta}{\sin^2\theta} \left(\frac{a^2}{r^2} - 2\right)\right]. \end{aligned} \tag{93}$$

The time-average Poynting vector for $r > a$ is obtained on setting $\Delta = 0$ in eq. (93).

However, the calculation (93) for the Poynting vector for $r < a$ includes a term in $\langle S_r \rangle$ of order $\Delta$ that varies as $1/r^4$. This is unphysical, and indicates that our approximations are not sufficiently reliable for $r < a$ for a detailed understanding of the energy flow there.

To the extent that we can ignore this blemish, our calculations confirm the expectation that for a center-fed antenna made of perfect conductors, the energy flows radially outward from the feed point.

This simple conclusion is agreeable, but perhaps not entirely intuitive. The existence of oscillating currents in the conductors of the antenna implies that at every point on its surface there are accelerating charges. These charges radiate energy, so we might expect to find a nonzero value of the time-average Poynting vector emanating from all points on the surface of the antenna. The requirement that the electric field be perpendicular to the surface of a perfect conductor leads to a coherence of the radiation of the charges such that no radiation appears to come from the bulk of the surface.

We are left with the possibility that radiation appears to come from the boundary of the perfect conductor. In the present example, the boundary includes the tips of the cones, and their ends at $r = a$. Popular cartoons of radiation from an antenna often show the radiation as emanating from the ends of the antenna, rather than its center. However, we find no evidence that Maxwell's equations lead to radiation from the ends of a simple center-fed antenna.

### 2.4.5 Appendix: Radial Variation of Currents and Voltages on Finite Length Cones

We claim that for finite-length, perfectly conducting cones, the current $I(r,t)$ and the voltage $V(r,t)$ are sinusoidal functions of $kr$.

The forms (74) and (76) certainly satisfy the claim.

The claim can be established by recalling eq. (17) for the radial component of the electric field, which must vanish on the surface of the perfectly conducting cones,

$$E_r(r,\theta_0,t) = 0 = \frac{i}{k}\frac{\partial^2 A_r(r,\theta_0,t)}{\partial r^2} + ikA_r(r,\theta_0,t). \tag{94}$$

Writing $A_r(r,\theta_0,t) = f(r)e^{-i\omega t}$, we have,

$$\frac{d^2 f}{dr^2} = -k^2 f, \tag{95}$$

which implies that $f$, and hence $A_r(r,\theta_0,t)$, is a sinusoidal function of $kr$.

Recalling eq. (16) which relates the voltage to the vector potential, $ikV = \partial A_r/\partial r$, we have at once that the voltage $V(r,\theta_0,t)$ on the cones is a sinusoidal function of $kr$.

As in eq. (76), the radial current $I$ on the surface of the cone follows from Ampère's law and eq. (9) as,

$$I(r,t) = \frac{cr\sin\theta_0 B_\phi(r,\theta_0,t)}{2} = -\frac{c\sin\theta_0}{2}\frac{\partial A_r(r,\theta_0,t)}{\partial\theta}. \tag{96}$$

At a given angle $\theta$, the derivative $\partial A_r(r,\theta,t)/\partial\theta$ has the same functional dependence on radius $r$ as does $A_r(r,\theta,t)$. Thus, the current $I(r,t)$ on the surface of the cones is a sinusoidal function of $kr$ (times $e^{-i\omega t}$).

In sec. 2.1 of [4], we show that the voltage and current distribution is also sinusoidal on the surface of thin perfectly conducting wires.

We now suppose that the cones have only a finite length $r = a$. In this case the current $I(r)$ must vanish at $r = a$. In principle, if the cones are solid there could be small polar currents on the spherical caps of the cones, or if the cones are hollow there could be a small radial current on the interior of the cones. For small cone angle $\theta_0$ these currents are negligible, so we adopt the condition,

$$I(r = a, t) = 0, \tag{97}$$

for cones of length $a$.

If we know the current $I(0)e^{-i\omega t}$ at the tip of the cones of length $a$, then the current $I(r,t)$ has the form,

$$I(r,t) = I(0)\sin[k(a-r)]e^{-i\omega t}. \tag{98}$$

# References


[1] H. Hertz, *The Forces of Electrical Oscillations Treated According to Maxwell's Theory*, Weidemann's Ann. **36**, 1 (1889); reprinted in chap. 9 of H. Hertz, *Electric Waves* (Dover, New York, 1962). A translation by O. Lodge appeared in Nature **39**, 402 (1889), http://physics.princeton.edu/~mcdonald/examples/EM/hertz.pdf

[2] K.T. McDonald, *Radiation in the Near Zone of a Hertzian Dipole* (April 22, 2004), http://physics.princeton.edu/~mcdonald/examples/nearzone.pdf

[3] K.T. McDonald, *Radiation in the Near Zone of a Small Loop Antenna* (June 7, 2004), http://physics.princeton.edu/~mcdonald/examples/smallloop.pdf

[4] K.T. McDonald, *Radiation in the Near Zone of a Center-Fed Linear Antenna* (June 21, 2004), http://physics.princeton.edu/~mcdonald/examples/linearantenna.pdf

[5] J.H. Poynting, *On the Transfer of Energy in the Electromagnetic Field*, Phil. Trans. Roy. Soc. London **175**, 343 (1884), http://physics.princeton.edu/~mcdonald/examples/EM/poynting_ptrsl_175_343_84.pdf

[6] S.A. Schelkunoff and H.T. Friis *Antennas: Theory and Practice* (Wiley, 1952), http://physics.princeton.edu/~mcdonald/examples/EM/schelkunoff_friis_52.pdf

[7] S.A. Schelkunoff, *Electromagnetic Waves* (Van Nostrand, 1943), http://physics.princeton.edu/~mcdonald/examples/EM/schelkunoff_waves_43.pdf

[8] W.R. Smythe, *Static and Dynamic Electricity*, 3rd ed. (McGraw-Hill, 1968), http://physics.princeton.edu/~mcdonald/examples/EM/smythe_50.pdf

[9] J.D. Jackson, *Classical Electrodynamics*, 3rd ed. (Wiley, 1999), http://physics.princeton.edu/~mcdonald/examples/EM/jackson_ce3_99.pdf

[10] P.M. Morse and H. Feshbach, *Methods of Theoretical Physics*, Vol. 1 (McGraw-Hill, 1953), http://physics.princeton.edu/~mcdonald/examples/EM/morse_feshbach_v1.pdf

[11] M. Abramowitz and I.A. Stegun, *Handbook of Mathematical Functions* (Nat. Bureau of Standards, 1964), http://physics.princeton.edu/~mcdonald/examples/EM/abramowitz_and_stegun.pdf

[12] J.A. Stratton, *Electromagnetic Theory* (McGraw-Hill, New York, 1941), http://physics.princeton.edu/~mcdonald/examples/EM/stratton_electromagnetic_theory.pdf